

3 Tesla Sodium Inversion Recovery Magnetic Resonance Imaging Allows for Improved Visualization of Intracellular Sodium Content Changes in Muscular Channelopathies

Armin Michael Nagel, PhD,* Erick Amarteifio, MD,†‡ Frank Lehmann-Horn, MD,§ Karin Jurkat-Rott, MD,§
Wolfgang Semmler, MD, PhD,* Lothar R. Schad, PhD,¶ and Marc-André Weber, MD†‡

Objectives: To implement different sodium (^{23}Na)-magnetic resonance imaging (MRI) contrasts at 3 Tesla and to evaluate if a weighting toward intracellular sodium can be achieved, using 2 rare muscular channelopathies as model diseases.

Materials and Methods: Both lower legs of 6 patients with hypokalemic periodic paralysis (HypoPP), 5 patients with paramyotonia congenita (PC), and 5 healthy volunteers were examined on a 3 Tesla system with 3 different ^{23}Na -MRI pulse sequences. HypoPP and PC are rare muscle diseases, which are well characterized by elevated myoplasmic sodium at rest and after cooling, respectively. Intra- and interindividual comparisons were performed before and after provocation of one lower leg muscle. Three different ^{23}Na -MRI sequences were applied: (i) The total tissue sodium concentration was measured using a spin-density sequence (^{23}Na -TSC). (ii) A T1-contrast was applied to assess whether the known changes of the intracellular sodium concentration can be visualized by T1-weighting (^{23}Na -T1). (iii) An inversion recovery (^{23}Na -IR) sequence was used to utmost suppress the sodium signal from extracellular or vasogenic edema. Furthermore, a potential influence of the temperature dependency of the sodium relaxation times was considered. Additionally, ^1H -MRI was performed to examine potential lipomatous or edematous changes.

Results: In HypoPP, all ^{23}Na sequences showed significantly ($P < 0.05$) higher signal intensities compared with PC patients and healthy subjects. In muscles of PC patients, provocation induced a significant ($P = 0.0007$) increase ($>20\%$) in the muscular ^{23}Na -IR signal and a corresponding decrease of muscle strength. Additionally, a tendency to higher ^{23}Na -T1 ($P = 0.07$) and ^{23}Na -TSC ($P = 0.07$) signal intensities was observed. Provocation revealed no significant changes in ^1H -MRI. In volunteers and in the contralateral, not cooled lower leg, there were no significant signal intensity changes after provocation. Furthermore, the ^{23}Na -IR sequence allows for a suppression of signal emanating from intravascular sodium and vasogenic edema.

Conclusions: Our results indicate that the ^{23}Na -IR sequence allows for a weighting toward intracellular sodium. The combined application of the ^{23}Na -TSC and the ^{23}Na -IR sequence enables an improved analysis of pathophysiological changes that occur in muscles of patients with muscular channelopathies.

Key Words: sodium, magnetic resonance imaging, projection reconstruction, channelopathies, muscle diseases

(Invest Radiol 2011;XX: 000–000)

Received February 8, 2011; accepted for publication (after revision) May 12, 2011.

From the Departments of *Medical Physics in Radiology and †Radiology, German Cancer Research Center (DKFZ), Heidelberg, Germany; ‡Department of Diagnostic and Interventional Radiology, University Hospital Heidelberg, Heidelberg, Germany; §Division of Neurophysiology, University of Ulm, Ulm, Germany; and ¶Computer Assisted Clinical Medicine, University of Heidelberg, Mannheim, Germany.

Conflicts of interest and sources of funding: none declared.

Reprints: Armin Michael Nagel, PhD, Department of Medical Physics in Radiology, German Cancer Research Center (DKFZ), Im Neuenheimer Feld 280, 69120 Heidelberg, Germany. E-mail: a.nagel@dkfz.de.

Copyright © 2011 by Lippincott Williams & Wilkins
ISSN: 0020-9996/11/0000-0001

Sodium ions (Na^+) play an important role in cell ion homeostasis and cell viability.¹ In healthy tissue, the extracellular Na^+ concentration ($[\text{Na}^+]_{\text{ex}} = 145 \text{ mM}$) is about 10-fold higher than the intracellular concentration ($[\text{Na}^+]_{\text{in}} = 10\text{--}15 \text{ mM}$).² Sodium (^{23}Na) magnetic resonance imaging (MRI) allows volume- and relaxation-weighted measurements of these Na^+ compartments, noninvasively. Thus, ^{23}Na -MRI is a promising diagnostic tool, because many pathologic processes alter this cellular ion distribution. Consequently, ^{23}Na -MRI has been applied for several organs such as brain (tumor^{3–6} and ischemia^{7,8}), kidney,⁹ heart,^{10–12} cartilage,^{13,14} and muscle.^{15–19}

In most previous ^{23}Na -MRI studies of pathologic processes, either the total tissue Na^+ concentration was measured or a T₁-weighted approach was used to increase the signal-to-noise ratio (SNR). However, a selective assessment of the intra- or extracellular Na^+ might be more indicative for the underlying pathologic process. Shift reagents allow for such a separation between intra- and extracellular Na^+ ,²⁰ but cannot be applied in humans because of their toxicity. Noninvasive techniques like multiple quantum filtering^{21,22} allow for a selective measurement of Na^+ with restricted mobility, but suffer from low SNR. Furthermore, it has been demonstrated in experiments with animals²³ and on the healthy human brain²⁴ that Na^+ with a longitudinal relaxation time equivalent to that of cerebrospinal fluid can be selectively suppressed with an inversion recovery (IR) sequence. The results from in vitro and animal studies suggest a weighting of the image toward intracellular Na^+ .²³ However, it remains unclear whether the proposed ^{23}Na -IR-imaging technique leads to an intracellular weighting in clinical applications.²⁴

Unfortunately, there is a lack of suitable phantoms that would allow a reliable modeling of in vivo conditions. Furthermore, there is no gold standard that can be applied in humans and that allows for clear in vivo separation between intra- and extracellular Na^+ . On the other hand, there are well-characterized muscular diseases that can be used as clinical model. These rare diseases are appropriate for establishing a new method because the patients have a clearly defined genotype and clinical phenotype with typical and reproducible trigger mechanisms.²⁵ In contrast, frequent diseases are caused by various etiologies. Therefore, patients with confirmed paramyotonia congenita (PC) were chosen as a clinical model. PC is characterized by a stiffening of the muscles during exercise or exposure to cold, which can merge into flaccid weakness that may last several hours even when the muscles were rapidly rewarmed.²⁵ The underlying pathogenetic mechanism is the gating defect of a Na^+ channel, causing a long-lasting depolarizing Na^+ inward current.²⁵ The resulting elevated intracellular Na^+ levels lead to membrane depolarization and weakness.²⁵ Because these pathologic effects can be easily provoked by cooling with high reproducibility¹⁸ and good correlation of in vivo ^{23}Na signal changes after provocation with membrane depolarization measured in muscle biopsies in these patients,¹⁷ the applied ^{23}Na -MRI techniques were compared before and after local provocation. Additionally, a second

group of patients suffering from confirmed hypokalemic periodic paralysis (HypoPP) was chosen. HypoPP presents as recurrent episodes of generalized flaccid weakness triggered by carbohydrate-induced hypokalemia and permanent progressive weakness with elevated myoplasmic resting Na^+ .²⁶ In both the diseases, transmembrane voltage-gated Na^+ (Nav1.4 in PC and HypoPP2) or calcium (Cav1.1 in HypoPP1) channels are affected by mutations. Because the muscles of the patients can be affected by edema or fatty infiltrations,^{16,18} both intra- and interindividual comparisons were performed. In particular, a comparison to healthy controls and measurements before and after provocation were accomplished.

The known intracellular Na^+ changes in PC and HypoPP patients were used to evaluate, if a weighting of the image toward intracellular Na^+ can be achieved. Thus, 3 different ^{23}Na -MRI sequences were applied. (i) A T1-weighted gradient echo sequence (^{23}Na -T1) was used to assess a potential change in longitudinal relaxation times after provocation. (ii) An IR sequence (^{23}Na -IR) was applied to reduce Na^+ signal emanating from edema and to yield a strong T1-weighting. (iii) The tissue Na^+ concentration (^{23}Na -TSC) was measured. Furthermore, the potential influence of a temperature dependency of the sodium relaxation times was considered. Additionally, ^1H -MRI was performed to examine potential lipomatous or edematous changes.

The aim of this work was to evaluate, if the applied ^{23}Na -MRI techniques are capable of providing a strong weighting toward the intracellular Na^+ and can be applied as a diagnostic tool for muscular channelopathies.

METHODS

Participants

Six patients (3 women, 3 men, mean age: 48 ± 23 years) with genetically confirmed HypoPP, 5 patients with genetically confirmed PC (5 men, mean age: 34 ± 14 years), and 5 healthy volunteers (3 women, 2 men, mean age: 29 ± 4 years) participated in this study. To avoid superimposition of the provocative effects of local cooling by systemic effects such as hypokalemia due to a heavy glucose-insulin load, the HypoPP patients were advised not to ingest a carbohydrate-rich meal before or between the 2 subsequent measurements. All healthy volunteers had full muscle strength at physical examination, revealed no evidence for muscular disorders and presented regular findings in ^1H MRI. The study was approved by the local review board and conducted according to the declaration of Helsinki. All participants gave written and oral informed consent before enrolment.

Magnetic Resonance Imaging

All examinations were performed on a 3 Tesla whole-body MR system (Magnetom Tim Trio, Siemens Healthcare, Erlangen, Germany). Images were acquired using a double-resonant (32.59 MHz/123.2 MHz) birdcage coil (Rapid Biomed GmbH, Rimpf, Germany). Three different ^{23}Na -MRI techniques based on a 3D density adapted projection reconstruction sequence²⁷ were used. Image reconstruction was performed offline with Matlab (Mathworks, Natick, MA). A Kaiser-Bessel gridding kernel was used,²⁸ followed by Hanning-filtering and a conventional Fast Fourier Transformation.

First, T₁-weighted ^{23}Na images were acquired with the following parameters: TE/TR = 0.25/6 milliseconds; $\alpha = 40^\circ$; voxel size: $5 \times 5 \times 5 \text{ mm}^3$; 14000 projections; 4 averages; total acquisition time: $T_{\text{AQ}} = 5$ minutes 36 seconds (^{23}Na -T1). Second, an IR sequence was used to suppress ^{23}Na -signal emanating from Na^+ in unrestricted environments (eg, saline [NaCl] solution). The following parameters were used: TE/TR = 0.3/124 milliseconds; TI = 34 milliseconds; voxel size: $6 \times 6 \times 6 \text{ mm}^3$; 5000 projections; 10 minutes 20 seconds (^{23}Na -IR). Third, relaxation weighting was

minimized using a short echo time (TE = 0.2 milliseconds) and a long repetition time (TR = 100 milliseconds) to measure the local tissue Na^+ concentration (^{23}Na -TSC). The following parameters were used: $\alpha = 90^\circ$; 5000 projections; voxel size: $5 \times 5 \times 5 \text{ mm}^3$; 8 minutes 20 seconds. Two reference tubes containing 51.3 mM Na^+ were used. Reference tube 1 contains pure saline (NaCl) solution, and reference tube 2 additionally contains 5% agarose gel. Signal intensities were calculated using linear extrapolation and reference tube 2. Reference tube 1 served as a control for the desired signal suppression in ^{23}Na -IR imaging.

In 10 consecutive slices, regions-of-interest (ROIs) were placed in both lower legs and the reference tubes by a radiologist and a physicist in consensus blinded to clinical data. Average ^{23}Na signal intensity values of each leg and reference tube were calculated. ROIs were selected in the ^{23}Na -TSC images and automatically transferred to the same positions in the other ^{23}Na -MRI data sets, to prevent a biased selection.

To evaluate muscular pathologic conditions, ^1H -MRI was performed in addition to ^{23}Na -MRI. A T1-weighted spin-echo sequence (TE/TR = 12/70 milliseconds) was used to detect potential lipomatous changes of muscle tissue. To examine possible edematous muscular changes, a T2-weighted short TI IR (STIR) sequence was applied (TE/TR = 65/6920 milliseconds; TI = 220 milliseconds). ^1H signal normalization was performed to reference tube 2. Grading into severe (++) , mild (+), and no lipomatous and edematous muscular degeneration (0) was performed by an experienced radiologist. Both legs were examined. For one PC patient (patient 7), ^1H -MRI had to be performed with a different coil, due to problems with the ^1H channel of the double-resonant birdcage coil. For this patient, no ^1H signal normalization was performed.

Examination Protocol

Both lower legs were examined simultaneously and the position of the legs was marked, to reproduce the positions for the following measurements. The provocation scheme was as follows¹⁸: Between the first and second measurement, 1 leg was cooled for 25 minutes with ice-water bags wrapped around the lower leg. The contralateral leg was not cooled and served as reference. Directly after cooling, the subjects had to dorsiflect their feet against resistance and stand on their tiptoes. The exercise lasted for approximately 2 minutes. Afterward the MRI examination was repeated. Before each measurement, the muscle strength was scored on a 6-point scale according to the grading system proposed by the British Medical Research Council: score of 0, complete paralysis; 1, minimal contraction; 2, active movement with gravity eliminated; 3, weak contraction against gravity; 4, active movement against gravity and resistance; and 5, normal strength. The same examination protocol was applied to patients and healthy volunteers. Additionally, 3 PC patients underwent a third MRI scan to examine the ^{23}Na -MRI signal evolution over a longer period of time. This measurement was started approximately 50 minutes (patient 7), 1 hour 50 minutes (patient 8), and 1 hour 40 minutes (patient 11) after the end of the provocation, respectively.

Evaluation of the Temperature Dependence of Na^+ Relaxation Times

Probes containing Na^+ in saline solution and Na^+ in agarose gel (5%) were measured at different temperatures. To assess T1 and T2 relaxation times, the free induction decay of the whole probe was measured. T1 relaxation was assessed using an IR sequence with the following parameters: TE = 0.3 milliseconds, TR = 600 milliseconds. TI was varied from 2 to 300 milliseconds in steps of 2 milliseconds. For the measurement of T2 relaxation times, a spin echo sequence was applied. TE was varied from 2 to 40 milliseconds in steps of 2 milliseconds for the agarose gel probe and from 2 to 228 milliseconds in steps of 6 milliseconds for the probe containing saline solution

(TE/TR = 0.3/300 milliseconds). A least square fitting routine was applied to calculate T1 and T2 relaxation times. All T1 relaxation times and the T2 relaxation time of the saline solution were calculated by monoexponential models. To assess the T2 relaxation time of Na⁺ in agarose gel, a biexponential model with a signal decay composed of 60% short (T2s) and 40% long (T2l) relaxation components was applied, based on the relaxation theory of spin 3/2 nuclei.²⁹ To quantify the temperature dependence of the Na⁺ relaxation times, a linear regression was applied to the data according to Eq. (1). T_x describes the relaxation time and T the temperature of the probe. The parameters m and c were calculated using linear regression. Equation 1 serves only as phenomenological description.

$$T_x = mT + c \quad (1)$$

Additionally, the influence of a potential temperature decrease (ΔT) on the signal intensities of the applied ²³Na sequences was simulated for 2 simple models. For the models, the temperature dependency of the T1 relaxation time of Na⁺ in saline solution (M1) and Na⁺ in 5% agarose gel (M2) was used. Equations 2 (²³Na-IR) and 3 (²³Na-TSC and ²³Na-T1) were applied. A starting temperature of 37°C (T = 310 K) was used, and the influence of the Boltzmann distribution to the signal was considered. Cooling can lead to a decrease of T2 (Fig. 5) and thus also to a decrease of T2*, which could lead to a slight reduction of the signal intensities. These effects were neglected. So, the formulas can serve as an upper bound for the signal increase.

$$Signal_{23Na-IR} = (1 - 2e^{-T1/T1}) + e^{(TR/T1)} \frac{e^{-\Delta E/k_B T}}{e^{k_B(T-\Delta T)}} \approx (1 - 2e^{-T1/T1}) + e^{(TR/T1)} \frac{T}{T - \Delta T} \quad (2)$$

$$Signal_{23Na-T1, 23Na-TSC} = \frac{1 - e^{(TR/T1)}}{(1 - e^{(TR/T1)} \cos(\alpha))} \frac{e^{-\Delta E/k_B T}}{e^{k_B(T-\Delta T)}} \approx \frac{1 - e^{(TR/T1)}}{(1 - e^{(TR/T1)} \cos(\alpha))} \frac{T}{T - \Delta T} \quad (3)$$

Statistical Analysis

Data were analyzed by using a 2-sided parametric *t* test for testing no difference versus difference and by using an one-sided *t* test for testing no difference against larger or smaller (level of significance, *P* = 0.05). Results were expressed as means ± standard deviation. Statistical testing was performed in MATLAB (The Mathworks, Natick, MA).

RESULTS

At rest, average Na⁺ concentrations (²³Na-TSC) of 24 ± 2 mM (healthy subjects), 27 ± 3 mM (PC patients), and 33 ± 5 mM (HypoPP) were measured. Relative signal intensities and measured Na⁺ concentrations are shown in Figure 1 and Table 1. *P* values obtained from 1- and 2-sided *t* tests are shown in Table 2. For the different measurements, no significant changes were observed for the noncooled (reference) leg (Fig. 1A–D). As expected,²⁶ the HypoPP patients showed significantly (*P* < 0.05) higher ²³Na-signal intensities compared with PC patients and healthy subjects (Fig. 1A–D). Also, ¹H-T2-STIR signal intensities of both patient groups were significantly higher compared with healthy volunteers (Table 2, e). After provocation, a significant ²³Na-IR signal increase (Fig. 1F, Table 2) and a corresponding decrease of the muscle strength (Table 1) was observed for PC patients. PC patients also showed a tendency to higher ²³Na-T1 (Fig. 1E, *P* = 0.07) and ²³Na-TSC (Fig.

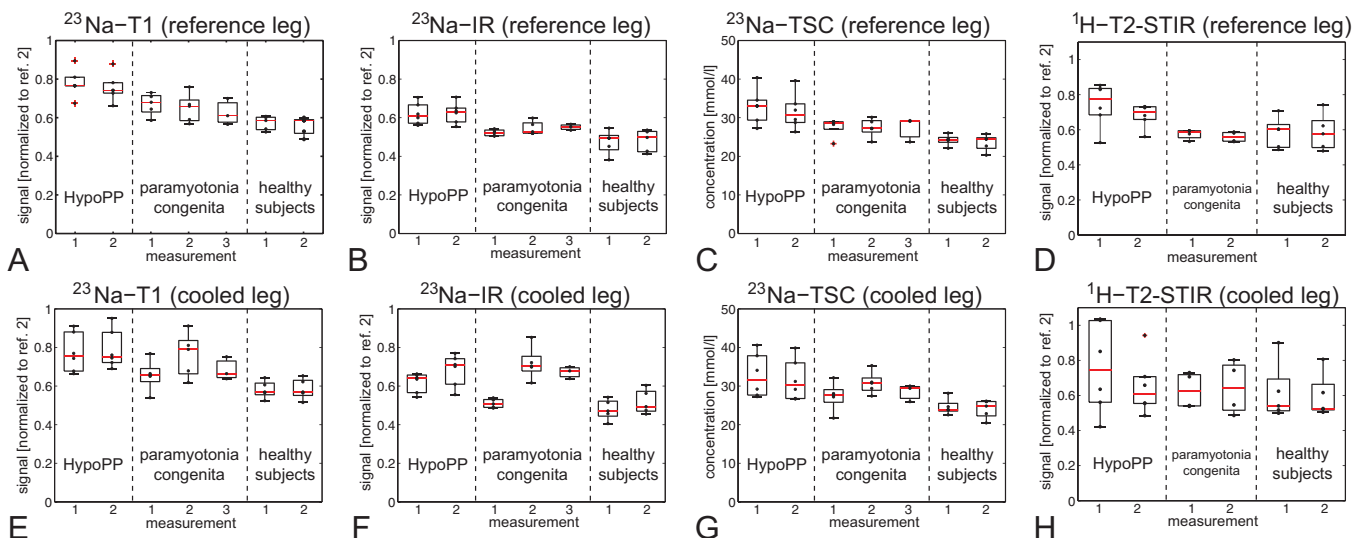


FIGURE 1. Measured signal intensities of patient and volunteer examinations before (first measurement) and after provocation (second and third measurement). Outliers (as identified by the *t* test) are indicated by crosses. Signal normalization was performed to reference tube 2 (ref. 2). The results obtained from the noncooled leg (reference leg) showed no significant changes between the different measurements (A–D). The HypoPP patients exhibited higher Na⁺ concentrations (C) and higher ²³Na-T1 and ²³Na-IR signal intensities than the healthy subjects. This signal increase is related to the degree of edematous muscular changes (D). The provoked leg (E–H) revealed a distinct signal increase in particular for PC patients and the ²³Na-IR measurement, whereas no significant changes were observed for T2-weighted proton imaging.

TABLE 1. Measured Muscle Strength of the Reference (re.) and the Cooled Lower Leg (co.) Immediately Before the Measurements

No	Disease	Age/Sex	Measurement 1 Strength		Measurement 2 Strength		Average Signal				Signal Change					
			re.	co.	re.	co.	T1 (a.u.)	IR (a.u.)	TSC (mM)	¹ H-T2 (a.u.)	T1 (%)	IR (%)	TSC (%)	¹ H-T2 (%)	¹ H-MRI Lip.	Ed.
1	HypoPP CaV1.1	23/f	5	5	5	4	0.9	0.63	40	0.93	+4	+17	-2	-8	0	++
2	HypoPP CaV1.1	60/m	5	4	5	4	0.82	0.61	35	0.94	0	+20	-5	-32	++	++
3	HypoPP NaV1.4	46/m	5	5	5	5	0.75	0.68	29	0.64	+2	+7	0	-1	0	+
4	HypoPP CaV1.1	17/m	5	5	5	5	0.68	0.66	27	0.47	+2	+7	-2	+14	0	0
5	HypoPP CaV1.1	69/f	5	5	5	5	0.79	0.56	34	0.83	-3	-2	-8	-23	++	+
6	HypoPP CaV1.1	71/f	5	5	5	4	0.72	0.57	30	0.66	+9	+13	-4	-12	++	+
7	PC NaV1.4	20/m	5	5	5	1	0.56	0.5	22	0.57	+26 (+23)	+44 (+40)	+26 (+20)	+1	0	0
8	PC NaV1.4	22/m	5	5	5	4	0.67	0.5	29	n.a.	+25 (+15)	+47 (+43)	+11 (+7)	n.a.	0	0
9	PC NaV1.4	53/m	5	5	5	4	0.75	0.54	31	0.62	+19	+58	+10	+14	+	0
10	PC NaV1.4	42/m	5	5	5	4	0.69	0.53	28	0.75	+19	+33	+13	+8	+	+
11	PC NaV1.4	35/m	5	5	5	4	0.65	0.51	28	0.66	-6 (-3)	+21 (+26)	+6 (+6)	+2	+	+
12	Volunteer	29/f	5	5	5	5	0.58	0.48	24	0.55	0	+8	-4	+4	0	0
13	Volunteer	36/m	5	5	5	5	0.62	0.51	27	0.56	-3	+9	-8	-1	0	0
14	Volunteer	28/m	5	5	5	5	0.61	0.54	24	0.57	+8	+11	+10	-6	0	0
15	Volunteer	25/f	5	5	5	5	0.52	0.39	22	0.51	-2	+12	-9	+2	0	0
16	Volunteer	26/f	5	5	5	5	0.55	0.46	25	0.56	0	+1	+1	-7	0	0

The muscle strength was scored on a 6-point scale according to the grading system proposed by the British Medical Research Council: score of 0, (complete paralysis) to score 5 (normal strength). The averaged signal intensities were measured before provocation. Normalization was performed on reference tube 2. The concentrations (TSC) are given in mM. Signal changes between measurement 1 and 2 are given for the cooled leg in percent. Changes larger than 10% (T1 and TSC) and 15% (IR, ¹H-T2) are printed in bold characters. For patients 7, 8, and 11, a third ²³Na measurement was performed. Signal changes relative to measurement 1 are given in brackets. Lipomatous and edematous muscular changes were graded into severe (++), mild (+), and no degeneration (0).

1G, $P = 0.07$) signal intensities after provocation, whereas no significant changes were observed for ¹H-T2-STIR imaging (Fig. 1H; Table 2, a–d). HypoPP patients and healthy subjects showed no relevant changes after provocation in ²³Na-T1 and ²³Na-TSC imaging (Fig. 1E, G; Table 1), whereas ²³Na-IR (Fig. 1F) imaging revealed a pronounced signal increase (>15%) for the 2 HypoPP patients, which exhibited severe muscular edema (patients 1 and 2; Table 1). Also, the healthy subjects showed a slight, but not significant, tendency for higher ²³Na-IR signal after provocation (Table 1, $P = 0.15$). Provocation did not affect the muscle strength of healthy subjects, whereas a decrease of the muscle strength was observed in 2 of 6 HypoPP patients and in all PC patients (Table 1). No relevant signal changes were observed in ¹H-T2-STIR imaging (Fig. 1H) for all groups.

Exemplary, the ¹H- and ²³Na-MR images of a healthy subject (No. 16) are shown in Figure 2. Muscle tissue of healthy subjects showed average SNR values of 13 ± 1 (²³Na-T1), 10 ± 1 (²³Na-IR), and 19 ± 1 (²³Na-TSC). Images of a HypoPP and a PC patient are shown in Figures 3 and 4. ²³Na-IR imaging allowed for a suppression of signal emanating from intravascular Na⁺ (Fig. 2, arrows) and also for a reduction of signal emitted from vasogenic edema (Fig. 3, arrows).

Edematous areas, which were also visible in the ¹H T2-STIR images, led to an elevated Na⁺ concentration and to hyperintensity in the ²³Na-T1 images (Fig. 3). ²³Na-T1 imaging led only to a slight reduction of signal which emanated from edema (Fig. 3). In contrast to healthy subjects and HypoPP patients, all PC patients exhibited a distinct (>20%) ²³Na-IR signal increase after provocation and also a tendency to a higher Na⁺ concentration (Table 1). The ²³Na-IR signal increase is most pronounced in the soleus and tibialis anterior muscles (Fig. 4). The third measurement, which was performed for 3 patients (7, 8, and 11), revealed a long-lasting ²³Na-IR-signal increase (Fig. 1F and Table 1). No changes were visible in proton imaging (Fig. 4).

The measured Na⁺ relaxation times for Na⁺ in saline solution and Na⁺ in agarose gel are plotted for different temperatures in Figure 5. The Na⁺ relaxation times of saline solution were more affected by temperature changes than those of agarose gel. The parameters obtained from linear regression are shown in Table 3 and were used to estimate the influence of a potential temperature change in muscle tissue on the ²³Na-IR signal intensity (Fig. 6). According to the applied models, temperature decreases of 7.5°C (model M1) and 13.6°C (model M2) lead to a ²³Na-IR signal increase of 50%.

TABLE 2. P Values Obtained From a One-Sided *t* Test (a, c) for Testing No Difference Against Larger or Smaller and a Two-Sided Parametric *t* Test (b, d) for Testing No Difference Versus Difference

	Reference Leg				Cooled Leg			
	T1	IR	TSC	¹ H-T2	T1	IR	TSC	¹ H-T2
a One-sided <i>t</i> test								
HypoPP	0.2869	0.4445	0.3172	0.1602	0.3889	0.0681	0.359	0.1602
PC	0.3194	0.1038	0.4594	0.4016	0.0658	0.0004	0.0718	0.4016
Volunteer	0.3041	0.4323	0.289	0.3653	0.4617	0.1539	0.3486	0.3653
b Two-sided <i>t</i> test								
HypoPP	0.5738	0.889	0.6345	0.3204	0.7778	0.1362	0.7179	0.4165
PC	0.6389	0.2077	0.9187	0.8032	0.1317	0.0007	0.1436	0.5699
Volunteer	0.6082	0.8646	0.5779	0.7306	0.9234	0.3079	0.6971	0.5928
	Measurement 1				Measurement 2			
	T1	IR	TSC	¹ H-T2	T1	IR	TSC	¹ H-T2
c One-sided <i>t</i> test								
HypoPP	0.4614	0.4719	0.4802	0.9113	0.2461	0.0923	0.4972	0.676
PC	0.3824	0.1837	0.4551	0.8032	0.0523	0.0015	0.0411	0.5649
Volunteer	0.3611	0.452	0.3629	0.9033	0.2133	0.1729	0.3673	0.8395
d Two-sided <i>t</i> test								
HypoPP	0.8032	0.9438	0.9605	0.9113	0.4922	0.1845	0.9945	0.676
PC	0.7647	0.3674	0.9101	0.7639	0.1047	0.003	0.0822	0.288
Volunteer	0.7222	0.9041	0.7259	0.9033	0.4267	0.3457	0.7346	0.8395
	One-Sided <i>t</i> Test				Two-Sided <i>t</i> Test			
	T1	IR	TSC	¹ H-T2	T1	IR	TSC	¹ H-T2
e								
HypoPP/vol.	0.0003	0.0007	0.003	0.0064	0.0006	0.0015	0.0061	0.0129
PC/vol.	0.0203	0.0861	0.049	0.0031	0.0406	0.1722	0.098	0.0062
HypoPP/PC	0.0168	0.0008	0.043	0.1885	0.0336	0.0015	0.0861	0.377

Significant values (*P* < 0.05) are printed in bold characters. (a, b) The level of significance was tested between measurement 1 and measurement 2. (c, d) The comparisons between reference and cooled leg were performed within a single measurement. (e) *P* values obtained from testing healthy subjects against HypoPP and PC patients and HypoPP against PC patients. The average signal intensities before provocation were considered.

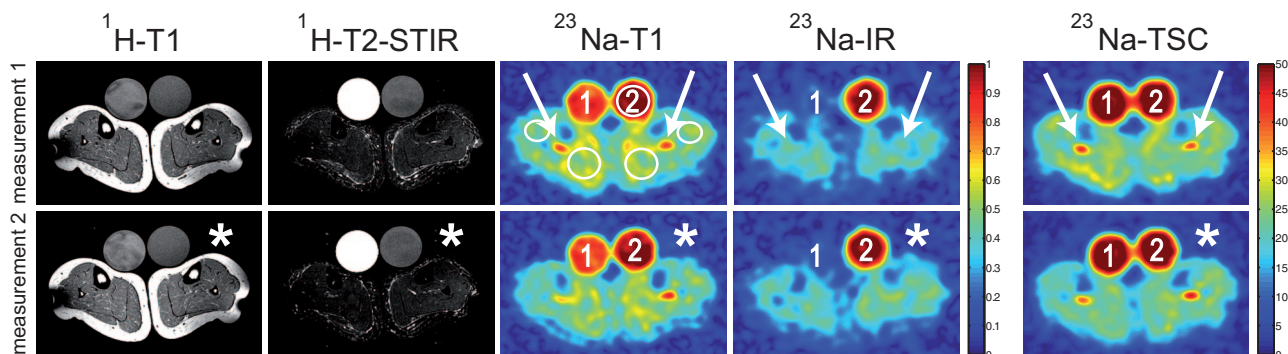


FIGURE 2. Transversal ¹H-MR and ²³Na-MR images of the lower legs of a healthy female subject (patient 16) before (measurement 1) and after provocation of the left lower leg muscle (*, measurement 2). Signal intensities of ²³Na-T1 and ²³Na-IR imaging were normalized to reference tube 2 (51.3 mM NaCl and 5% agarose gel). The ²³Na-TSC signal intensities are given in mM. Note that reference tube one (pure 51.3 mM saline solution) shows no signal intensity in ²³Na-IR imaging. The positions of the ROIs are shown, exemplarily. The signal emanating from intravascular sodium ions is suppressed in ²³Na-IR imaging (arrows). In ²³Na-T1 imaging reference tube one shows also reduced signal intensity compared with reference tube 2 (5% agarose gel). Fat and bone exhibits lower signal intensities compared with muscle tissue in all 3 ²³Na-MRI sequences. After provocation (*) no distinct signal change is visible for all sequences.

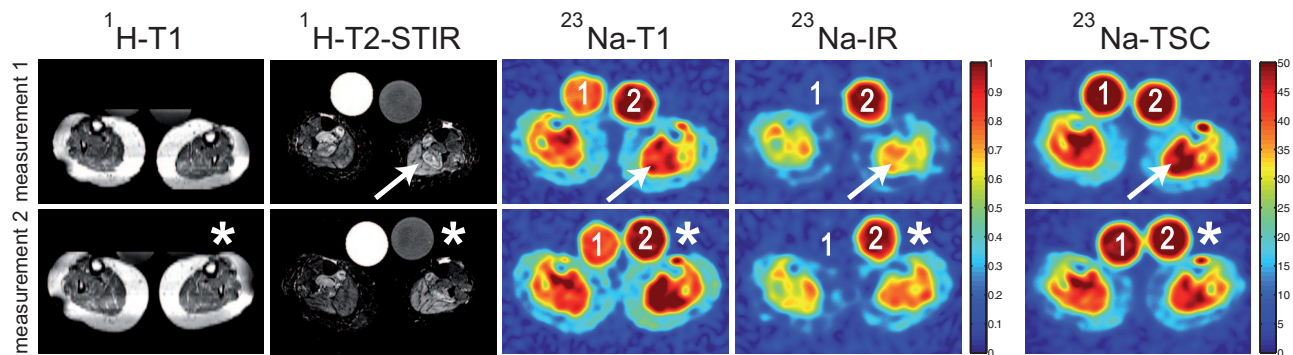


FIGURE 3. ^1H -MR and ^{23}Na -MR images of the lower legs of a female HypoPP patient (patient 1) before (measurement 1) and after provocation of the left lower leg (*, measurement 2). Edematous muscular changes (arrows), which are visible in ^1H T2-STIR imaging exhibit a high Na^+ concentration and also high signal intensities in ^{23}Na -T1 imaging. ^{23}Na -IR imaging reveals reduced signal intensity compared with ^{23}Na -T1 and ^{23}Na -TSC imaging, but shows still higher signal intensity than in healthy muscle (Fig. 2). After provocation (*), the ^{23}Na -IR sequence in particular shows an increased muscular signal intensity in the cooled leg. The ^{23}Na -TSC signal remains unchanged. Note the minor quality of ^1H T1-TSE imaging due to reformatting of coronal images.

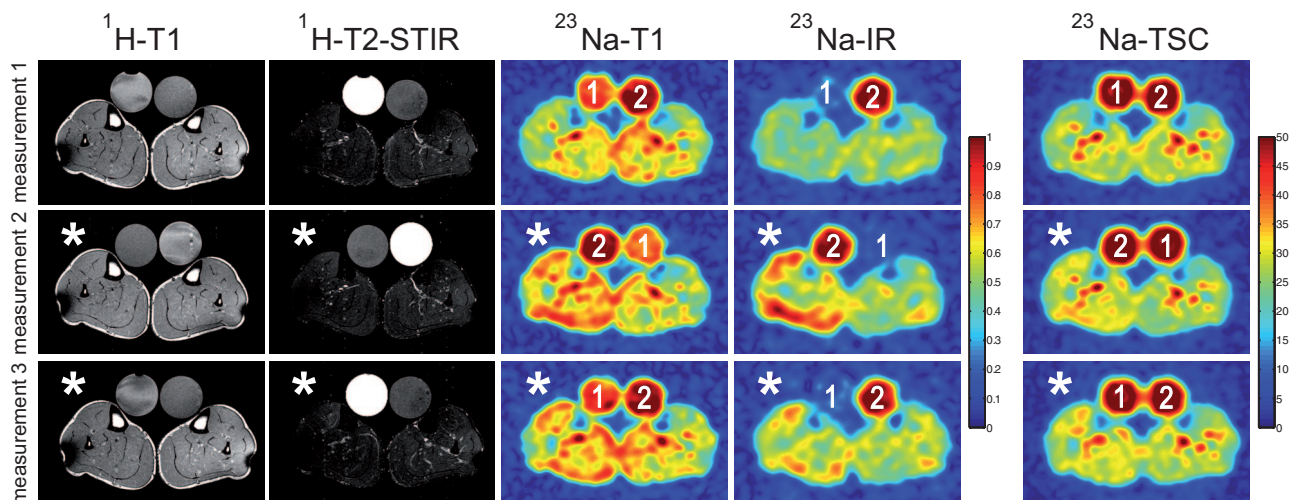


FIGURE 4. ^1H -MR and ^{23}Na -MR images of a PC patient (patient 7). ^1H -MRI revealed no pathologic signal changes before and after provocation. The cooled leg (*) showed a distinct muscular ^{23}Na -signal increase in ^{23}Na -T1 and ^{23}Na -IR imaging, as well as a slight increase in the total Na^+ concentration (^{23}Na -TSC), when compared with measurement 1 and the nonprovoked leg. Slight ^{23}Na -signal increases are still visible in measurement 3 (110 minutes after provocation). The increase is most pronounced in ^{23}Na -IR imaging.

DISCUSSION

Because there are no phantoms that allow a reliable modeling of in vivo conditions with different intra- and extracellular sodium concentrations, patients with well characterized rare muscular channelopathies have been chosen as clinical model. It is known, that in muscles of PC patients exposure to cold leads to a transient increase of the intracellular Na^+ concentration that in turn induces a reversible muscles weakness.²⁵ The latter was observed for all PC patients after provocation (Table 1), which is in good agreement with previous observations.¹⁸ Therefore, it can be assumed, that the examined PC patients exhibit an intracellular sodium accumulation in the provoked leg.

Our results and the known pathophysiology of PC²⁵ indicate that the application of ^{23}Na -IR imaging allows for a visualization of the intracellular Na^+ accumulation in muscles of patients with channelopathies that are present with no pathologic findings or only mildly degenerated muscles in ^1H -MRI. The observed ^{23}Na -IR

signal increase might be caused by shorter T1 relaxation times in the intracellular space compared with extracellular Na^+ compartments. Shorter T1 relaxation of intracellular sodium compared with extracellular sodium were also measured previously in the perfused frog and rat hearts.³⁰ Because the applied ^{23}Na -IR sequence is heavily T1-weighted, a weighting of the signal toward intracellular Na^+ is expected. This is also in good accordance with the tendency of an increased ^{23}Na -T1 signal intensity and the tendency of an increase in the total Na^+ concentration. The latter can be explained by the expectation that the extracellular Na^+ concentration remains virtually constant as long as adequate perfusion of the tissue can be provided and that the intracellular Na^+ concentration increases. The less pronounced signal increase for the ^{23}Na -T1 sequence, when compared with the ^{23}Na -IR sequence, can be explained with the fact that the latter provides stronger T1-weighting. Furthermore, in ^{23}Na -TSC and ^{23}Na -T1 imaging vasoconstriction after cooling might counter signal increases because of the increase in intracel-

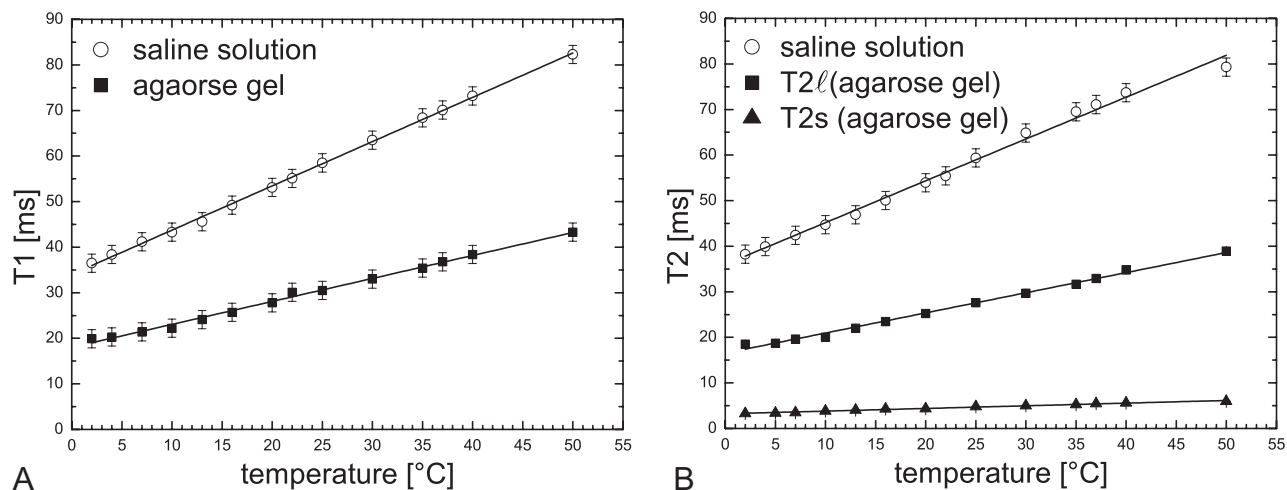


FIGURE 5. T1 (A) and T2 (B) relaxation times of Na^+ in saline solution and agarose gel for different temperatures. For T1 relaxation and T2 relaxation of Na^+ in saline solution, a monoexponential fit was applied to calculate the relaxation times. For T2 relaxation of Na^+ in agarose gel, a biexponential model with a short component T2s and a long component T2l was used. Linear regression was applied to the calculated relaxation times. The slopes are given in Table 3. The temperature dependence of the relaxation times is more pronounced for Na^+ in saline solution than for Na^+ in agarose gel.

TABLE 3. Parameters Obtained From Linear Regression According to Equation 1

	m(T1) (ms/°C)	c(T1) (ms)	m(T2x) (ms/°C)	c(T2x) (ms)
Saline solution	0.971 ± 0.009	34.0 ± 0.2	0.92 ± 0.02	36.0 ± 0.6
Agarose gel	0.50 ± 0.01	18.0 ± 0.3	(l) 0.442 ± 0.005 (s) 0.058 ± 0.002	(l) 16.5 ± 0.2 (s) 3.22 ± 0.05

The corresponding plots can be found in Figure 5. The parameters for long and short relaxation components are indicated by (l) and (s), respectively. Na^+ relaxation times of pure saline solution are more affected by a temperature change than the relaxation times of agarose gel.

lular sodium. In contrast, the ^{23}Na -IR sequence suppresses signal from blood vessel (Fig. 2), and thus better emphasizes the intracellular component.

A putative temperature effect might contribute to the ^{23}Na -IR signal increase, but seems to be insufficient to explain the marked increase, because healthy subjects, who show similar results in ^1H -MRI, did not exhibit a comparable signal increase. This is substantiated by the fact that the muscles of PC patients showed a tendency to an increase in the total Na^+ concentration (Table 1) and a long-lasting ^{23}Na -IR signal increase. Similar to the more pronounced temperature dependence of the T1 relaxation times of Na^+ in saline solution when compared with Na^+ in agarose gel (Table 2), the Na^+ relaxation times of edema should be more affected by a temperature change than the relaxation times of healthy muscle tissue. Thus, a slight temperature decrease could have a more pronounced effect to the ^{23}Na -IR signal in muscle tissue of these 2 HypoPP patients whose muscles were severely affected by edema (Table 1; patients 1 and 2) compared with those patients with muscle tissue that is not or only mildly affected by edema.

In previous ^{23}Na -MRI studies on muscular channelopathies,^{16–18} sequences comparable to ^{23}Na -T1 were applied and also revealed signal increases at rest¹⁶ and after provocation,^{17,18} which is in good accordance with our study. Our observed Na^+ concentrations of healthy muscle tissue measured by TSC ^{23}Na -MRI are in accordance with other studies.^{19,31} For future studies, we suggest the

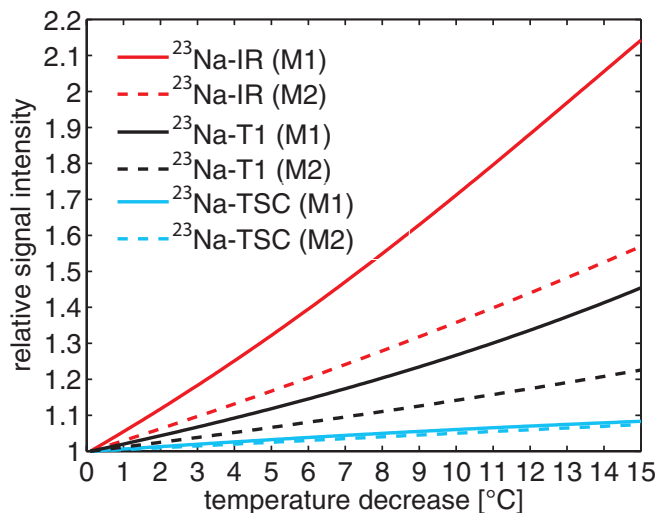


FIGURE 6. Simulated influence of a temperature decrease on the applied ^{23}Na -MR sequences for 2 simple models. The models differ in the applied temperature dependence of the Na^+ relaxation times. For model M1, the temperature dependence of Na^+ in saline solution ($m = 0.971$ ms/°C) was used and for model M2 the temperature dependence of Na^+ in agarose gel ($m = 0.50$ ms/°C) was applied (Table 3 and Fig. 5). In both models, a T1 relaxation time of 29 milliseconds was assumed. This value was obtained from patient 11, using an inversion recovery sequence that measures the average of the free induction decay of both lower leg muscles (reference tubes were omitted for this measurement). The ^{23}Na -IR sequence is more sensitive to potential temperature changes than ^{23}Na -T1 or ^{23}Na -TSC imaging.

application of ^{23}Na -IR and ^{23}Na -TSC imaging, because the combined application of these sequences allows both, the evaluation of a change of the total Na^+ concentration and a potential change of T1 relaxation times. Although, ^{23}Na -T1 exhibits higher SNR-efficiency

when compared with ^{23}Na -IR imaging, we suggest the application of the latter sequence, because it revealed a more pronounced signal increase in the muscles of PC patients after provocation. Furthermore, ^{23}Na -IR imaging reduces background signal of blood vessels (Fig. 1) and muscular edema (Fig. 2) that might hamper the correct interpretation of conventional ^{23}Na -images. The better sensitivity of the ^{23}Na -IR sequence compared with ^{23}Na -T1 imaging should also allow for better monitoring of therapy effects, for example, the application of Na^+ channel blockers such as mexiletine.¹⁸ Additionally, in future studies that include cooling, an in vivo measurement of the temperature is desirable to estimate the contribution of a potential temperature change to the ^{23}Na -IR signal intensities. Furthermore, the application of more dedicated coils and higher magnetic field strengths might improve image quality in future studies.³²

One of the limitations of our study is that only an indirect proof of the correlation between the measured ^{23}Na -IR increase and an intracellular Na^+ accumulation was provided, because there is no gold standard that allows a noninvasive measurement of the intracellular Na^+ concentration in humans. The assumption that the intracellular Na^+ concentration is increased in the cooled leg of PC patients after provocation is based on the well-known physiology of PC²⁵ and the observed decrease in muscle strength (Table 1). Furthermore, the ^{23}Na -IR sequence was optimized to suppress signal from reference tube one, since exact values of intra- and extracellular T1 relaxation times are not available. An exact knowledge of these relaxation times would allow a more appropriate choice of the inversion time and might allow an even better image contrast. A further limitation is the low number of subjects, which is caused by the fact that HypoPP and PC are rare diseases (prevalence $\leq 1:100,000$), which makes patient recruitment difficult.

CONCLUSION

Our results indicate that the ^{23}Na -IR sequence provides a strong weighting toward intracellular sodium and allows a better visualization of intracellular sodium content changes than the ^{23}Na -T1 or ^{23}Na -TSC sequences. The combined application of the ^{23}Na -TSC and the ^{23}Na -IR sequence enables an improved analysis of pathophysiological changes that occur in muscles of patients with muscular channelopathies.

ACKNOWLEDGMENT

Frank Lehmann-Horn is endowed Senior Research Professor for Neurosciences of the non-profit Hertie-Foundation.

REFERENCES

- Boada FE, Laverde G, Jungreis C, et al. Loss of cell ion homeostasis and cell viability in the brain: what sodium MRI can tell us. *Curr Top Dev Biol*. 2005;70:77–101.
- Hilal SK, Ra JB, Oh CH, et al. Sodium Imaging. In: Stark DD, Bradley WG, eds. *Magnetic Resonance Imaging*. St Louis, MO: C.V. Mosby;1988:715–729.
- Ouwerkerk R, Bleich KB, Gillen JS, et al. Tissue sodium concentration in human brain tumors as measured with ^{23}Na MR imaging. *Radiology*. 2003;227:529–537.
- Thulborn KR, Davis D, Adams H, et al. Quantitative tissue sodium concentration mapping of the growth of focal cerebral tumors with sodium magnetic resonance imaging. *Magn Reson Med*. 1999;41:351–359.
- Weber MA, Henze M, Tutenberg J, et al. Biopsy targeting gliomas: do functional imaging techniques identify similar target areas? *Invest Radiol*. 2010;45:755–768.
- Nielsen-Vallespin S, Weber MA, Bock M, et al. 3D radial projection technique with ultrashort echo times for sodium MRI: clinical applications in human brain and skeletal muscle. *Magn Reson Med*. 2007;57:74–81.
- Thulborn KR, Davis D, Snyder J, et al. Sodium MR imaging of acute and subacute stroke for assessment of tissue viability. *Neuroimaging Clin N Am*. 2005;15:639–653, xi-xii.
- Thulborn KR, Gindin TS, Davis D, et al. Comprehensive MR imaging protocol for stroke management: tissue sodium concentration as a measure of tissue viability in nonhuman primate studies and in clinical studies. *Radiology*. 1999;213:156–166.
- Maril N, Rosen Y, Reynolds GH, et al. Sodium MRI of the human kidney at 3 Tesla. *Magn Reson Med*. 2006;56:1229–1234.
- Jerecic R, Bock M, Nielsen-Vallespin S, et al. ECG-gated ^{23}Na -MRI of the human heart using a 3D-radial projection technique with ultra-short echo times. *Magma*. 2004;16:297–302.
- Konstandin S, Nagel AM, Heiler PM, et al. Two-dimensional radial acquisition technique with density adaption in sodium MRI. *Magn Reson Med*. 2011;65:1090–1096.
- Sandstede JJ, Hillenbrand H, Beer M, et al. Time course of ^{23}Na signal intensity after myocardial infarction in humans. *Magn Reson Med*. 2004;52:545–551.
- Borthakur A, Shapiro EM, Beers J, et al. Sensitivity of MRI to proteoglycan depletion in cartilage: comparison of sodium and proton MRI. *Osteoarthritis Cartilage*. 2000;8:288–293.
- Trattnig S, Welsch GH, Juras V, et al. ^{23}Na MR imaging at 7 T after knee matrix-associated autologous chondrocyte transplantation preliminary results. *Radiology*. 257:175–184.
- Kushnir T, Knubovets T, Itzhak Y, et al. In vivo ^{23}Na NMR studies of myotonic dystrophy. *Magn Reson Med*. 1997;37:192–196.
- Jurkat-Rott K, Weber MA, Fauler M, et al. K^+ -dependent paradoxical membrane depolarization and Na^+ overload, major and reversible contributors to weakness by ion channel leaks. *Proc Natl Acad Sci U S A*. 2009;106:4036–4041.
- Weber MA, Nielsen-Vallespin S, Essig M, et al. Muscle Na^+ channelopathies: MRI detects intracellular ^{23}Na accumulation during episodic weakness. *Neurology*. 2006;67:1151–1158.
- Weber MA, Nielsen-Vallespin S, Huttner HB, et al. Evaluation of patients with paramyotonia at ^{23}Na MR imaging during cold-induced weakness. *Radiology*. 2006;240:489–500.
- Constantinides CD, Gillen JS, Boada FE, et al. Human skeletal muscle: sodium MR imaging and quantification-potential applications in exercise and disease. *Radiology*. 2000;216:559–568.
- Winter PM, Bansal N. TmDOTP(5-) as a (^{23}Na) shift reagent for the subcutaneously implanted 9L gliosarcoma in rats. *Magn Reson Med*. 2001;45:436–442.
- Hancu I, Boada FE, Shen GX. Three-dimensional triple-quantum-filtered (^{23}Na) imaging of in vivo human brain. *Magn Reson Med*. 1999;42:1146–1154.
- Pekar J, Renshaw PF, Leigh JS. Selective detection of intracellular sodium by coherence-transfer NMR. *J Magn Reson* (1969). 1987;72:159–161.
- Kline RP, Wu EX, Petrylak DP, et al. Rapid in vivo monitoring of chemotherapeutic response using weighted sodium magnetic resonance imaging. *Clin Cancer Res*. 2000;6:2146–2156.
- Stobbe R, Beaulieu C. In vivo sodium magnetic resonance imaging of the human brain using soft inversion recovery fluid attenuation. *Magn Reson Med*. 2005;54:1305–1310.
- Lehmann-Horn F, Jurkat-Rott K. Voltage-gated ion channels and hereditary disease. *Physiol Rev*. 1999;79:1317–1372.
- Jurkat-Rott K, Holzherr B, Fauler M, et al. Sodium channelopathies of skeletal muscle result from gain or loss of function. *Pflugers Arch*. 2010;460:239–248.
- Nagel AM, Laun FB, Weber MA, et al. Sodium MRI using a density-adapted 3D radial acquisition technique. *Magn Reson Med*. 2009;62:1565–1573.
- O'Sullivan JD. A fast sinc function gridding algorithm for Fourier inversion in computer tomography IEEE transactions on medical imaging. 1985;MI-4:200–207.
- Hubbard PS. Nonexponential nuclear magnetic relaxation by quadrupole interactions. *J Chem Phys*. 1970;53:985–987.
- Foy BD, Burstein D. Interstitial sodium nuclear magnetic resonance relaxation times in perfused hearts. *Biophys J*. 1990;58:127–134.
- Bansal N, Szczepaniak L, Ternullo D, et al. Effect of exercise on ^{23}Na MRI and relaxation characteristics of the human calf muscle. *J Magn Reson Imaging*. 2000;11:532–538.
- Chang G, Wang L, Schweitzer ME, et al. 3D ^{23}Na MRI of human skeletal muscle at 7 Tesla: initial experience. *Eur Radiol*. 2010;20:2039–2046.